



Designing a three-dimensional alginate hydrogel by spraying method for cartilage tissue engineering

Jessica Tritz, Rachid Rahouadj, Natalia de Isla, Naceur Charif, Astrid Pinzano, Didier Mainard, Danielle Bensoussan, Patrick Netter, Jean-François Stoltz, Nadia Benkirane-Jessel, et al.

► To cite this version:

Jessica Tritz, Rachid Rahouadj, Natalia de Isla, Naceur Charif, Astrid Pinzano, et al.. Designing a three-dimensional alginate hydrogel by spraying method for cartilage tissue engineering. *Soft Matter*, 2010, 6 (20), pp.5165-5174. 10.1039/c000790k . hal-03697373

HAL Id: hal-03697373

<https://hal.science/hal-03697373>

Submitted on 21 Sep 2022

HAL is a multi-disciplinary open access archive for the deposit and dissemination of scientific research documents, whether they are published or not. The documents may come from teaching and research institutions in France or abroad, or from public or private research centers.

L'archive ouverte pluridisciplinaire **HAL**, est destinée au dépôt et à la diffusion de documents scientifiques de niveau recherche, publiés ou non, émanant des établissements d'enseignement et de recherche français ou étrangers, des laboratoires publics ou privés.

Designing a three-dimensional alginate hydrogel by spraying method for cartilage tissue engineering

Jessica Tritz* (1), Rachid Rahouadj* (2), Natalia de Isla (1), Naceur Charif (1), Astrid Pinzano (1), Didier Mainard (1,5), Danielle Bensoussan (1,4), Patrick Netter (1), Jean-François Stoltz (1,4), Nadia Benkirane-Jessel (3,5), Céline Huselstein (1)[#]

1 CNRS UMR 7561 and FR CNRS-INSERM 32.09 Nancy University, Vandœuvre-lès-Nancy 54500, France

2 CNRS UMR 7563 INPL, Vandœuvre-lès-Nancy 54500, France

3 INSERM UMR 977 and Faculté de Chirurgie Dentaire, Strasbourg 67000, France

4 CHU de Nancy, Unité de Thérapie Cellulaire et Tissulaire, 54000, France

5 Hôpital central, Service de Chirurgie Orthopédique, Nancy, 54000, France

* Contributed equally to this work

[#] E-mail: celine.huselstein@medecine.uhp-nancy.fr

Abstract

Cartilage tissue engineering strategies generally result in homogeneous tissue structures with little resemblance to native zonal organization of articular cartilage. The main objective of our work concerns the buildup of complex biomaterials aimed at reconstructing biological tissue with three dimensional cells construction for mimicking cartilage architecture.

In this first step, our strategy is based on structures formation by simple and progressive spraying of mixed alginate and chondrocytes at different pressures. We report the first demonstration of spraying effect on chondrocytes inside an alginate hydrogel at short (i) and long term (ii) and the mechanical behavior of sprayed hydrogel by biomechanical tests (Plane Strain Compression Tests).

Our results indicate clearly that during the first days of culture the cells were influenced by the construction method (spraying or molding, control method) with low viability and higher production level of nitrite. From day 7, the cell behaviors become similar for both methods. Indeed after 28 days of culture, type II collagen was observed, showing the cartilage gene expression, then a similar behavior for all methods. Finally, we conclude that the mechanical performances of sprayed hydrogels was enhanced compared to controls.

We report here for the first time that it is possible to spray mixed alginate and chondrocytes with weakly damage for cells. Therefore, the sprayed hydrogel keeps not only the mechanical properties needed for cells, but also maintains the chondrocyte phenotype to induce cartilage.

Keywords Tissue engineering – Cartilage – Spraying Cells – Alginate hydrogel – Mechanical behavior – Chondrocyte Phenotype

1. Introduction

For decades, the treatment of degenerative cartilage and bone diseases has been a challenge for orthopedic surgeons due to the apparent inability of cartilage and bone to repair themselves. There is no effective therapy available, and patients can only be helped by surgical joint replacement. An inherent major concern is the limited availability of autografts, which significantly reduces the number and the type of treatable defects. One of the goals of tissue engineering is to develop tools allowing the *in vitro* construction and mimicking of tissue architectures.¹

The articular cartilage is characterized by an organized depth-dependent structure containing embedded chondrocytes in extracellular matrix (ECM).² This stratified organization can be observed at each level, i.e. ECM composition, cell morphology, cytoskeleton and cell mechanical behavior.³⁻⁵ Physiological functions of the articular cartilage consist in transmitting movements and absorbing loads. Moreover, *in vivo* mechanical loadings stimulate different ECM synthesis by chondrocytes in order to adapt each layer to the local stress state.³

Most approaches in cartilage tissue engineering involve capture of cells *via* biodegradable scaffolds in homogeneous tissue structures.^{6,7} The architecture of these scaffolds, categorized into hydrogels, sponges and fibrous meshes, plays a crucial role in dictating the cellular behavior.⁶ Various ways are explored for the development of 3-D scaffolds interacting with cells.^{1, 8, 9} Different scaffolds have been used as for example as artificial extracellular matrix networks, nanofibrillar networks formed by self-assembly or hydrogel.⁹⁻¹² Recently, Hwang et al. reported the influence of biomaterial composition on the ECM production, by considering the zone in the cartilage, i.e. surface or deep zonal cells.¹³ Different kinds of hydrogels have been used for technological and biomedical applications that are a very attractive technology. Their water-swelling structure leads to a time-dependent release or incorporation of water molecules in the outer environment.¹⁴⁻¹⁷ Alginate hydrogel is a polymer largely employed for it is very easy to use in cartilage engineering.^{18,19} However, few investigations considered the organization of cartilage as a basis for the development of the stratified tissue engineering.^{7, 20, 21} From this viewpoint, complex 3-D structures of cartilage can *a priori* be built layer by layer using a large number of different components, including hydrogel with various cell types, drugs, proteins, peptides or DNA.²²⁻³⁷ However, up to now, few methodologies efficiently synthesizing stratified structures including viable specific cells interacting with a biofunctionalized environment has been proposed. Recent research has focused on cell sheet engineering, showing that the grown sheets may be easily extracted to obtain a subsequent tissue.³⁸ Recently, Matsusaki et al. have described the fabrication of cellular multilayers in a step-by-step process where cell sheets were alternated with polyelectrolyte layers - these later playing the role of nanometer-sized extracellular matrix.³⁹ However several limits rise from these techniques: complicated handling or lengthy constructions to mention only two of them. This is why, for future research, there is need to develop cellular active stratified materials.

An easily applicable technique that is able to deposit multiple cell types in 3-D without overt cellular damage is probably cell spraying.⁴⁰ Indeed, this deposition method has been previously used to spray keratinocytes on wounded skin to accelerate healing,⁴¹ melanocytes to restore skin color,⁴² bladder urothelial and smooth muscle cells to reconstitute colon segments.⁴³ We report here another approach based on the spraying of different elements of the extracellular matrix and cells in order to form a highly functionalized and structured biomaterial. The proposed way will allow the

control from the surface to the in-depth of the distribution of the different needed elements (matrix and cells). Recently, we have reported the spray formation of complex 3D multilayers, composed of alternating calcium-alginate gel domains containing cells and the multilayered polyelectrolyte film, containing active molecules as a reservoir for cells.³⁴ The sprayed mixed alginate gel and cells have been characterized by using not only fibroblastic cells as a model but also melanocytes. We have also shown that these sprayed cells remain still active and are able to express active receptors.³⁴ Our ultimate objective is to develop a new concept fundamentally based on the feasibility of building up organized construction respecting specific cell zones,^{13, 20, 44, 45} by spraying layer by layer each zone of the cartilage alternatively with polyelectrolyte to weld layers. By using this new approach, we can correlate each sprayed zonal material with different mechanical properties to induce different chondrocyte phenotype of stratified cartilage tissue. First, we have to adapt this new technology for the cartilage tissue engineering which needs a thick scaffold to repair the whole depth of cartilage instead of the actual scaffold done with this concept.

Thus, we constructed a 3D alginate hydrogel containing chondrocytes by simple and progressive spraying method. The aim of the present study was to evaluate this new approach on the mechanical and cellular level.

2. Material and methods

2.1. Cell isolation and culture

Chondrocytes were isolated enzymatically from the femoral head of male Wistar rats (10 weeks old) (Charles River, France). The maintenance and care of the experimental rats were in accordance with the guidelines of the NIH. In brief, cartilage tissue was digested in pronase at 2 mg mL⁻¹ (Sigma, France) in a 0.9% NaCl solution supplemented with Penicillin at 10 U mL⁻¹ /Streptomycin at 100 µg mL⁻¹ (P/S) and Amphotericin B (Amp) at 2.5 µg mL⁻¹ (Gibco, France). Then, cartilage was digested overnight in a collagenase B solution of 2 mg mL⁻¹ (Roche Applied Science, USA) in Dulbecco's Modified Eagles Medium (DMEM) without phenol red supplemented (Gibco, France) with P/S and Amp. The supernatant was centrifuged and cells were seeded at 13300 cells cm⁻² with complete medium (DMEM-F12 supplemented with 10% Fetal Bovine Serum (Gibco, France), P/S, Amp and 2 mM of Glutamine (Sigma, France)) in T-flasks treated by plasma for cells adhesion (BD Falcon, France). Chondrocytes were cultivated up to passage 1 (P1) and embedded in 1.5% alginate gel in P2.

2.2. Alginate gel preparation with or without cells (Fig. 1.a)

In this study, we used two methods for alginate gel construction. The objective was to test not only the behavior of cells embedded in these hydrogels but also their capacity to resist to compression stress.

- *Cells embedded in alginate solution*: Cells were seeded at 2.10⁶ cells mL⁻¹ in 1.5% sodium alginate solution (w/v in 0.9% NaCl solution, medium viscosity, Sigma, France) to have an alginate cellular suspension.

- *Molding construction*: The first type of construction was composed of sterile 1.5% alginate gel or cellular suspension injected into a mold. This approach is often used in cartilage bioengineering.^{46, 47} 1.5-2 mL of sterile 1.5% sodium alginate solution are injected into molds (thickness = 1.5 mm, diameter = 25 mm; Bern, Switzerland).⁴⁶ Then, molds were placed

horizontally in a petri dish and alginate suspension gelled when the CaCl_2 solution (102 mM) was added.

- *Spraying construction*: The second type of construction was based on the innovative process consisting in spraying 10 mL of 1.5% sodium alginate solution with or without cells. The spraying system was constituted by an airbrush working with a compressor, ⁴⁸ to induce spraying pressure being equal to 0.9 or 1.2 bar. The spraying bottle containing the alginate solution or cellular suspension in alginate was connected to the airbrush, and then solution was sprayed on a sterile glass plate. The gelling phase was realized by deeping quickly and horizontally the glass plate with the alginate gel in a bath of 102 mM CaCl_2 solution.

After 15min of gelation, whatever the process, biomaterials were washed twice with a 0.9% NaCl solution before being cut with a biopsy punch (5 mm diameter, Stiefel). Cylinders (with cells) were obtained for biological experiments and cultured during 14 or 28 days (Fig. 1.b) in a 48-well-plate, with complete medium supplemented by 1 mM of CaCl_2 to avoid hydrogel dissolution. The medium was changed twice in a week. Gels without cell were kept at +4°C before mechanical testing.

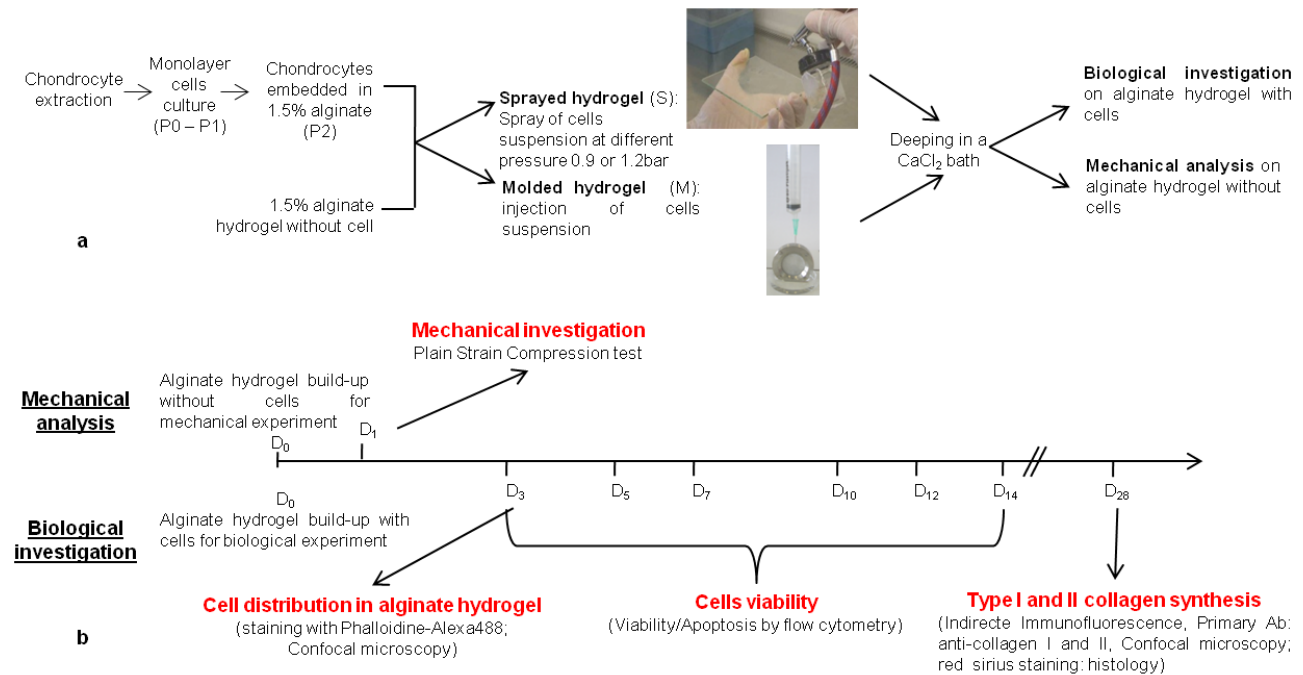


Figure 1. Schematic illustration of construction methods used (a) and experiments realized during the study (b).

2.3. Mechanical behavior of alginate gels

In this study, the biomaterials were built up in the form of thin sheets, which makes the use of traditional mechanical tests inadequate. Indeed, in the present case, the compression of cylindrical specimens of small dimensions (e.g. 1.4 mm of height and 2 mm of diameter, prepared from initial sheets of 1.4 mm of thickness) involves a maximum volume of matter of 4.4 mm³. This leads to a problem of precision in the evaluation of the mechanical parameters, in particular the stress response. Indeed, most of the mechanical procedures used for the characterization of alginate are based on relaxation and compression creep tests in small strains, performed under quasi-static or dynamic (cyclic) condition. For more details on the rheological models developed specifically for

alginate, one may refer to the review by Moresi et al. (considering relaxation, creep and complex properties in dynamic straining), or by Nussinovitch et al. (using modified Maxwell model).^{49, 50}

Our idea consisted in carrying out specific tests to characterize volumes of matter much more significant than for the uniaxial compression tests (approximately 6 times more, i.e. 157 mm³).

In fact, the Plane Strain Compression test, (PSC test), or the Watts-Ford test, usually used in metal forming and tribological simulation, was performed on 1.5% alginate gels, by either injection into mold (M) or spray (S), (see Fig. 2). Here the test consists in flattening an alginate strip (thickness $2h_0$) between two parallel anvils (width $2a$). The PSC test becomes useful when the sheet specimens are too thin and soft for a classical tensile test or for uniaxial compression. Moreover, it can give stress-strain curves up to considerably higher strains than tensile tests.

The lower anvil remained fixed, whereas the higher one is animated by a translation movement, $\delta(t)$, at controlled speed, $\dot{\delta}$, varying in the range 0.1 - 6 mm min⁻¹. From a mechanical point of view, it is well known that the generated plane strain state in such tests may be described using the corresponding equivalent Von Mises strain.^{51, 52} During the test, a load cell gives the force response $F(t)$ as a function of the displacement $\delta(t)$. From a classical modeling of the plastic deformation in the PSC test, it is also reported,⁵¹ that the equivalent Von Mises stress, $\bar{\sigma}$, and strain, $\bar{\epsilon}$, may be written as

$$\bar{\sigma} = \left[\frac{\frac{\sqrt{3}}{2}}{1 + \bar{m} \frac{a}{4(h_0 - \delta(t))}} \right] \frac{F(t)}{2aL_0}$$

$$\bar{\epsilon} = \frac{2}{\sqrt{3}} \ln \left(\frac{h_0}{h_0 - \delta(t)} \right)$$

where h_0 , L_0 , \bar{m} , are the initial thickness, the initial length and the friction factor, respectively.

All the PSC tests were carried out under isothermal condition (+20°C), and with negligible friction effect (estimated at $\bar{m} = 0.05$).

In this approach, the two alginate hydrogels making methods are tested and compared: spray at 0.9bar (S) vs. molding (M). The parameters which were taken into consideration were: alginate viscosity ($\mu = 45\text{-}60$ mPa.s), time of polymerization (15 min), conservation conditions (constant temperature +4°C, medium composition NaCl 0.9% + 10 mM CaCl₂). The sprayed specimens, of mean sizes $L_0 = 28$ mm and $2h_0 = 1.47 \pm 0.1$ mm, were cut from circular plates of 80 mm of diameter. The molded samples, of diameter 25 mm and thickness 1.62 ± 0.19 mm, were obtained by using directly the stainless steel mould as described previously.

The experimental stress-strain responses, obtained from 48 specimens (i.e. 24 for each process, and 6 per strain-rate level) provided at the same time the effect of preparation methods and of the strain-rate sensitivity.

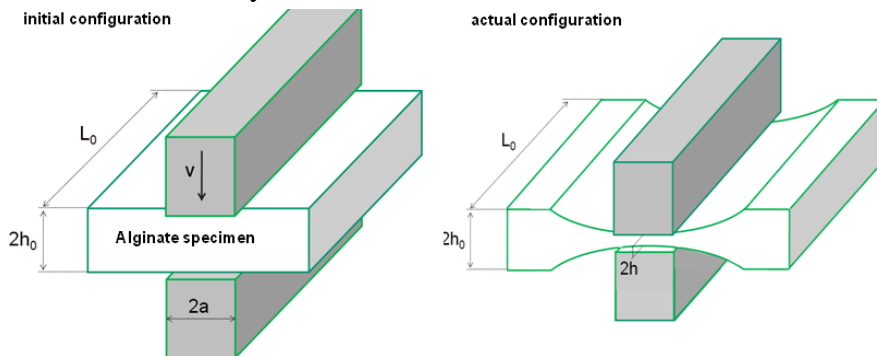


Figure 2. Schematic illustration of Plane Strain Compression test (PSC test) at velocity $\dot{\delta}$, with L_0 , the initial length, $2h_0$, the initial thickness and $2a$ the width.

2.4. Viability, apoptosis and necrosis analysis

Apoptosis and necrosis of cells were analyzed by flow cytometry using the Vybrant/Apoptosis™ kit based on Annexin V/Propidium Iodide staining procedure (Molecular Probes, France). Cells were taken off from alginate hydrogel by dissolution in 55 mM sodium citrate and 50 mM EDTA after 3, 7 and 14 days. After centrifugation (320g, 5 min), cells were suspended in 100 µL of 1X Annexin-lyant buffer (10 mM HEPES, 140 mM NaCl, 2.5 mM CaCl₂, pH 7.4) with 2.5 µL of Annexin V-Alexa 488 and 1 µL of Propidium Iodide (PI, 100 µg mL⁻¹), for 15 min at room temperature. After incubation, 200 µL of 1X Annexin V buffer were added to each sample. Then, cells were analyzed by the measurement of fluorescence emission at 530 nm and 575 nm, respectively for Alexa 488 and PI, with EPICS XL flow cytometer (Beckman Coulter). For all analyses, at least 5000 events were analyzed.

2.5. Measurement of Nitrite production

The basal nitrite (NO) production was measured as the amount of nitrite accumulated in the supernatants of cell culture when chondrocytes were embedded into the sprayed alginate biomaterial (0.9 and 1.2 bar). The Griess Reagent Kit (Molecular Probes, France) for NO determination was used to analyze nitrite amount after 1, 3, 5, 7, 10 and 14 days of culture. For each analyzed time point, supernatant of samples was centrifuged (5 min, 11 000g). The supernatant was then recovered and frozen at -20°C up to dosage. 150 µL of tested samples were added to 130 µL of deionized water in a 96-well-plate. A standard curve was drawn with 8 samples, ranging from 0.78 µM to 100 µM. Then, 20 µL of Griess reagent were added to samples which were incubated for 30 min. The absorbance was read at 548 nm with a spectrophotometer (Varioskan Flash, Thermo Scientific). Results were standardized with the quantity of DNA present in each biomaterial.

2.6. DNA content

Total DNA was determined by fluorimetric quantification. Chondrocytes were separated from alginate by dissolving the alginate buildup in 55 mM sodium citrate and 50 mM EDTA, pH 6.8. Total cellular DNA in the remaining part of sample digests was determined using Hoechst dye 33258 (Interchim, France). Calf thymus DNA in a solution of Phosphate Buffer Saline (PBS) was used for the preparation of the calibration curve, ranging from 0 to 0.5 µg mL⁻¹. Aliquots (standards or samples) were homogenized with 100 µL of Hoechst buffer (10 mM Tris, 0.1 mM NaCl at pH = 7.4), then 4 cycles of freezing (-80°C) and thawing (+37°C) were performed to lyse cells. Lastly, DNA solutions were mixed with 2 mL of 100 ng mL⁻¹ Hoechst 33258 fluorescent dye solution (Invitrogen, France) and read at excitation wavelength 356 nm, emission wavelength 458 nm with the spectrophotometer.

2.7. Cells distribution and type I and II collagen expression

After 3 and 14 days of culture, actin was labeled with Alexa Fluor 488 Phalloïdin (Invitrogen, France) to analyze both, cell repartition in the alginate 3D structure and in monolayer culture, and cytoskeleton morphology. First, samples were washed with PBS then fixed with 1% paraformaldehyde solution (Sigma, France). After cells permeabilization with 0.1% Triton X-100

solution (Sigma, France), Alexa Fluor 488 Phalloïdin is incubated for 20 min with samples. Finally, the samples were washed twice with DMEM without phenol red.

After 28 days, type I and II collagen synthesized by cells were analyzed by indirect immunofluorescence staining. Briefly, samples were washed three times with PBS, and then blocked with 0.5% bovine serum albumin (BSA) in DMEM without phenol red (named blocking solution) for 15 min. Specimens were incubated for 45 min with rabbit anti-rat type I or II collagen polyclonal antibodies (Calbiochem, France). After washing with blocking solution, samples were incubated (45 min) in the dark with secondary antibodies: a goat anti-rabbit IgG Alexa Fluor 488 (Molecular Probes, Netherland). After two washes, cylinders were fixed with 1% paraformaldehyde solution.

For all labelings, Alexa Fluor 488 fluorescence emission was detected using Confocal Laser Scanning Microscopy (CLSM). For the image series, a Leica TCS SP2 equipped with an acousto-optical beamsplitter (AOBS) was used. Excitation was achieved by the 488 nm line from an Argon laser for Alexa Fluor 488 labeling. All photomultipliers used were adjusted to the same sensitivity (gain/offset).

2.8. Total collagen synthesis

Alginate scaffolds were fixed in 4% paraformaldehyde in 100 mM sodium cacodylate containing 10 mM CaCl_2 at pH 7.4 during 4 hours and then washed overnight in 100 mM sodium cacodylate and 50 mM BaCl_2 buffer at pH 7.4 (the latter to irreversibly crosslink the alginate matrix). The scaffolds were dehydrated through a series of ethanol concentrations, cleared with toluene and embedded in paraffin wax. Sections were cut at a thickness of 5 μm using a sledge microtome and mounted on to glass slides. For histological examination, the sections were stained using Sirius red for collagen content. The observation of Sirius red in polarized light microscopy showed collagen organization inside the matrix.

2.9. Statistical analysis

All data are presented as means \pm standard error means (SEM) of three independent experiments. A second way ANOVA was used to determine if significant differences existed for the mixed-population experiment. A p -value less than 0.05 was considered significant for the ANOVAs. If significance existed, a post-hoc analysis was performed using the Tukey's multiple comparison tests to evaluate significance for all experiments.

3. Results and Discussion

3.1. Chondrocytes viability, distribution and nitrite production

a- Cell viability and nitrite production

Chondrocytes viability in sprayed gels was checked on a regular basis at different pressures, and was compared to cell viability in molded gels (Fig. 3a). The results indicated clearly that during the 3 first days of culture, the viability of sprayed cells was significantly smaller at 0.9 and 1.2 bar than for the molded cells (respectively $p < 0.01$, $p < 0.001$). After 3 days of culture, cell viability was increased ($>95\%$), whatever the pressure. Moreover, only necrotic cells were distinguish from apoptotic ones ($<1\%$) of death cells (data not shown).

It is well known that NO (nitrite) is highly produced by chondrocytes from OA-derived cartilage and that this is one of the molecules that triggers chondrocytes apoptosis and cartilage breakdown

via activating matrix metalloproteinase activity.⁵³ Thus, nitrite production could be considered as an indicator of the stress felt by chondrocytes. Therefore, we analyzed the daily nitrite production of sprayed (0.9 and 1.2 bar) and molded cells (Fig. 3b). It appeared that the daily nitrite production increased up to 3 days in the supernatants of engineered scaffolds, especially those of sprayed cells. After 3 days of culture, this production decreased and became homogeneous whatever scaffolds. Jeffrey *et al.* have shown that when chondrocytes were submitted to impact, their viability decreased with the increase of the impact energy.⁵⁴ If we consider the alginate hydrogel as an incompressible fluid, with the same spray angle, we could apply the Bernoulli equation. In this condition, energy is directly proportional to spray pressure. Indeed, between 0.9 and 1.2 bar, the impact energy of sprayed cells on glass plate increased of 33%. We can then suppose that, for pressures higher than 0.9 bar, the impact of cells on the support was caused injury and explained nitrite production during the first time of culture and caused cells death observed with necrotic cells. After 3 days of culture, it seems that cells were adapted to their environment without any detectable damage. These results clearly indicate that more than 80% of sprayed cells are still active and this method is weakly injurious compared to the control one.

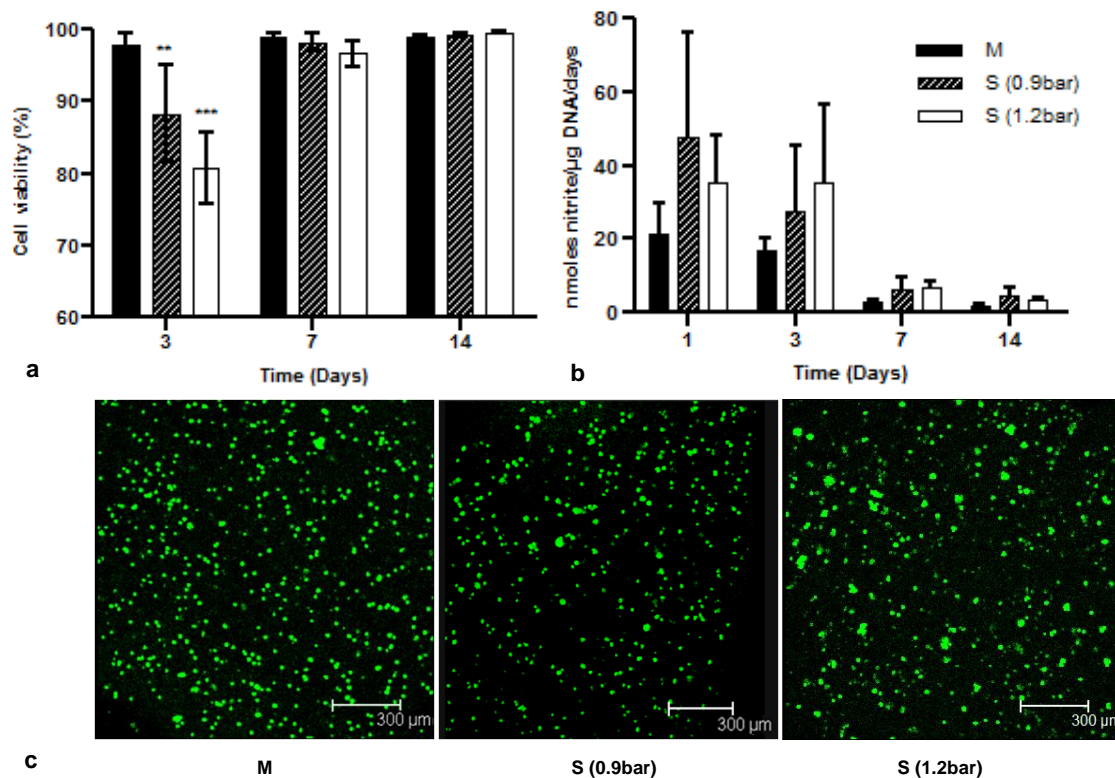
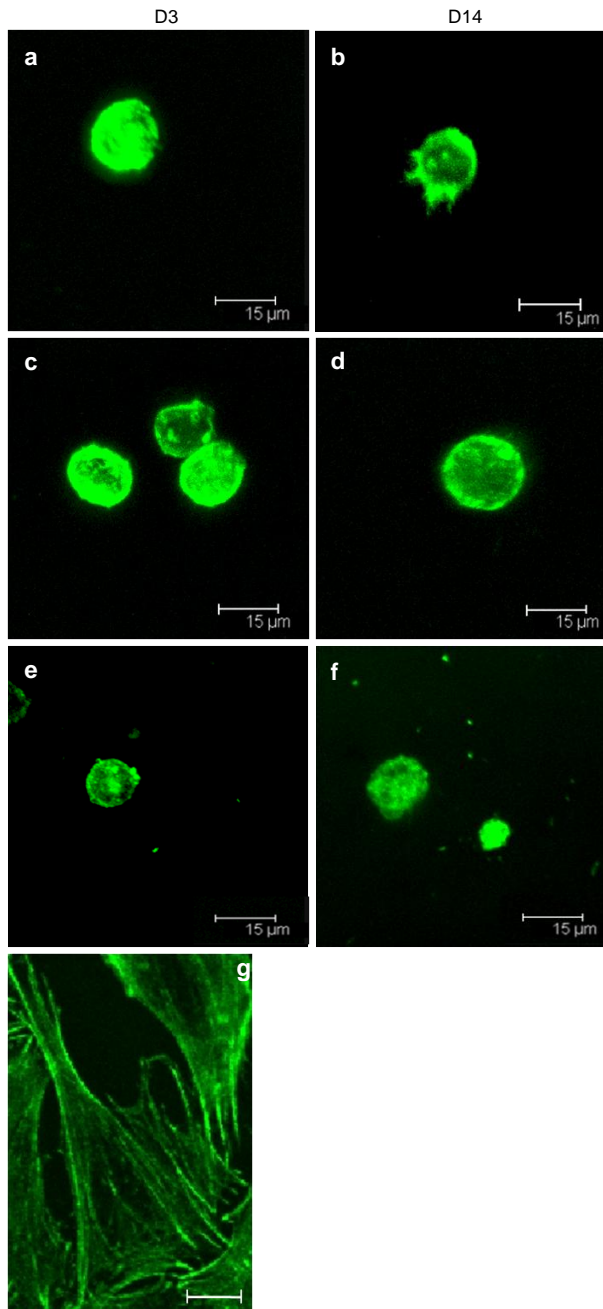


Figure 3. Effect of manufacturing process on mixed chondrocytes alginate hydrogel. Construction methods effect on viability of molded or sprayed (M, S) chondrocyte (a). The viability of sprayed (S) mixed chondrocytes and alginate was followed according to pressure and time of culture. The molded (M) chondrocytes and alginate was used as a control. Nitrite production was analyzed during a certain time (1, 3, 7, and 14 days of culture) on sprayed mixed chondrocyte and alginate at 0.9 and 1.2 bar of pressure and molded ones (b). All results were expressed in means \pm SEM, * p <0.05, ** p <0.01, *** p <0.001, D1 vs Dx. The cells distribution was observed by confocal visualization of actin after 3 days of culture in sprayed mixed Chondrocytes and alginate at 0.9, 1.2 bar or molded into the alginate gel as a control with more homogeneous distribution (c) (Leica SP2- AOBS, Obj X40, NO = 0.8).

b- Chondrocytes distribution in alginate hydrogel and actin distribution

Cell distribution in sprayed gel has been examined by confocal microscopy, (Fig. 3c). The results revealed clearly that for spraying at 1.2 bar, cell distribution was less homogeneous than for the molded cells. It may be due to the disappearance of dead cells (cf. §3.1.a, 20% of dead cells from D0 to D3 in sprayed gel at 1.2 bar). The cell distribution was also examined for spraying at 0.9 bar and revealed that at this pressure, chondrocytes distribution was as for molded cells.

To understand better sprayed cells behavior, we also analyzed the organization of F-actin filaments. As a checking, we have analyzed the organization of actin during monolayer expansion (Fig. 4g). In this kind of culture, chondrocytes have a fibroblastic-like shape and their width dimension was greater than that of chondrocytes in 3D culture. Actin formed stress fibers



predominantly located just beneath the cell membrane where the cells attached to the culture well substrate. Monolayer culture induces cell dedifferentiation into fibroblast-like cells which results in serious alterations in cytoskeleton architecture (Fig. 4g). In 3D system, on D3, chondrocytes had a spheroid shape and instead of stress fibers, actin adopted a punctuated organization and was distributed even beneath the cell membrane for sprayed mixed cells and hydrogel (Fig. 4c, 4e). However, in molded construction, the actin seems to be more diffused (Fig. 4a). On D14, we observed an identical actin distribution, whatever scaffold, with a punctuate cytoskeleton. Recently, Kino-oka *et al.*⁵⁵ reported the suppression of chondrocytes dedifferentiation through the disruption of the actin cytoskeleton which caused the punctuate F-Actin. These authors have also shown that this cytoskeleton disruption in round shaped cells facilitates the formation of collagen type II specific to chondrocyte and cartilage.

Figure 4. Confocal visualization of filamentous actin (F actin) distribution in chondrocytes during 3D (a to f) or monolayer culture (g, scale = 15 µm) culture. Actin visualization is observed, after 3 and 14 days of in 3D culture: molded chondrocytes into the alginate as a control (a, b) or sprayed mixed chondrocytes and alginate at 0.9 bar (c, d) or 1.2 bar (e, f) (Leica SP2-AOBS, Obj X40, NO=0.8).

3.2 Long term chondrocyte behavior between different construction methods

As type II collagen protein expression is the definitive indicator of the chondrogenic phenotype, we have analyzed the presence of this kind of collagen thanks to the sprayed cells expression in alginate hydrogel, after 28 days of culture. Type I collagen, a chondrocyte dedifferentiation indicator, and total collagen were also observed (Fig. 5). First, it appeared that total collagen synthesis and especially types I and II collagen was exclusively pericellular whatever the construction methods and sprayed pressure (Fig. 5). On the one hand, in molded hydrogels and sprayed ones at 0.9 bar, types I and II collagen were observed in this pericellular space. On the other hand, in sprayed hydrogels at 1.2 bar, type I was mainly observed (Fig. 5f and 5i). Moreover, we could also observe that sprayed constructions showed variation of height between 0.9 and 1.2 bar (1.47 ± 0.1 mm and 0.977 ± 0.17 mm, respectively; Fig. 5b and 5c). Previously, we reported the need to build thick scaffold for cartilage tissue engineering. Shepherd DE *et al.* shown that ankles and knees had a mean cartilage thickness in the ranges 1.0 to 1.62 mm and 1.69 to 2.55 mm respectively, while hips had a mean cartilage thickness in the range 1.35 to 2.0 mm.⁵⁶ The 1.2 bar pressure does not enable us to obtain this kind of thickness. By considering the type of collagen synthesized as well as the thickness which can be obtained, this kind of pressure will be excluded from the rest of our study.

Finally, mechanical properties of molded and sprayed alginate hydrogel (sprayed at 0.9 bar) without cells were evaluated to research if sprayed constructions are relevant for cartilage tissue engineering.

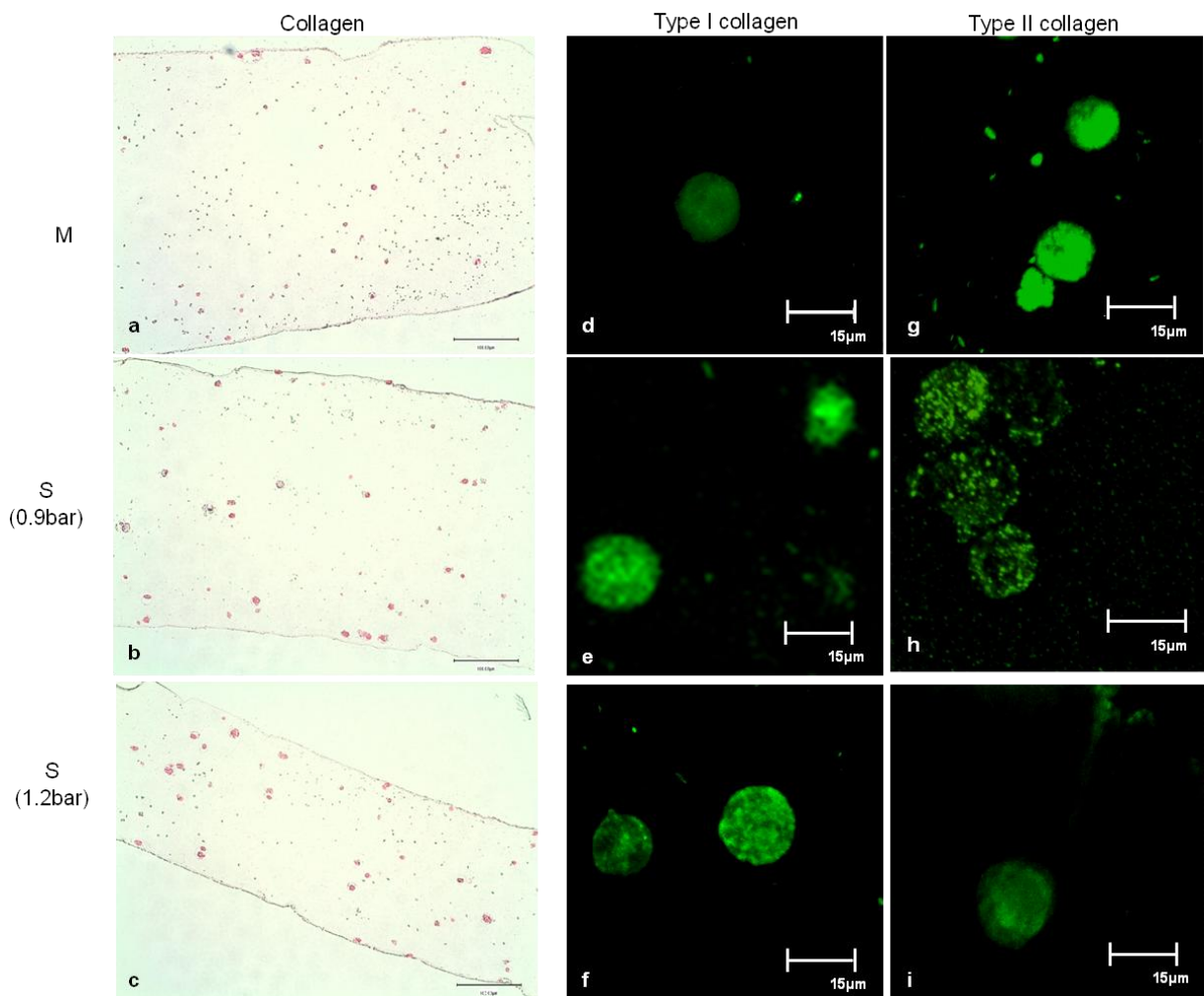


Figure 5. Collagen synthesis in alginate hydrogel constructs. Histological staining (red Sirius) allowed observing total collagen synthesis (a, b, c). Confocal microscopy visualization of types I and II collagen synthesized by sprayed mixed chondrocytes and alginate at 0.9 and 1.2 bar or molded ones (d to i), after 28 days of culture. Scale bars represent 100 μm for a, b, c images, and 15 μm for the fluorescent images.

3.3 Influence of the method on the mechanical behavior of the biomaterials

We further analyzed the mechanical properties of both sprayed and molded gel under quasi-static conditions. Thus, PSC tests have been performed for different experimental conditions: variable strain rates for the two preparation processes, (Fig. 6). The tridimensional stress state involved in the PSC test is closer to the true conditions observed *in vivo* than in the uniaxial compression test. In addition, this type of test allows exploring a wide range of deformations without any instability, as mentioned previously. Indeed, the strain range extends up to 80%, which largely contains the strain levels observed *in vivo* (12% maximum).⁵⁷ Fig. 6 does not only show the continuous increase of the equivalent strain-stress responses up to rupture, but it also shows a strain-rate dependence of the alginate hydrogels. One notice that the stress response was significantly higher for sprayed (S) specimens than for molded ones (M) whatever the controlled velocity (0.1, 0.6 and 6 mm min^{-1} , Fig. 6a, b and d respectively). For example, at an equivalent strain, $\bar{\epsilon} = 0.5$ and a velocity $\dot{\delta} = 0.6 \text{ mm min}^{-1}$, the equivalent stress $\bar{\sigma}$ was approximately 50 kPa for S specimens and 18 kPa for the M ones (Fig 6b). However at 2 mm min^{-1} , the stress seems to follow the same evolution for the two compared methods (Fig 6c).

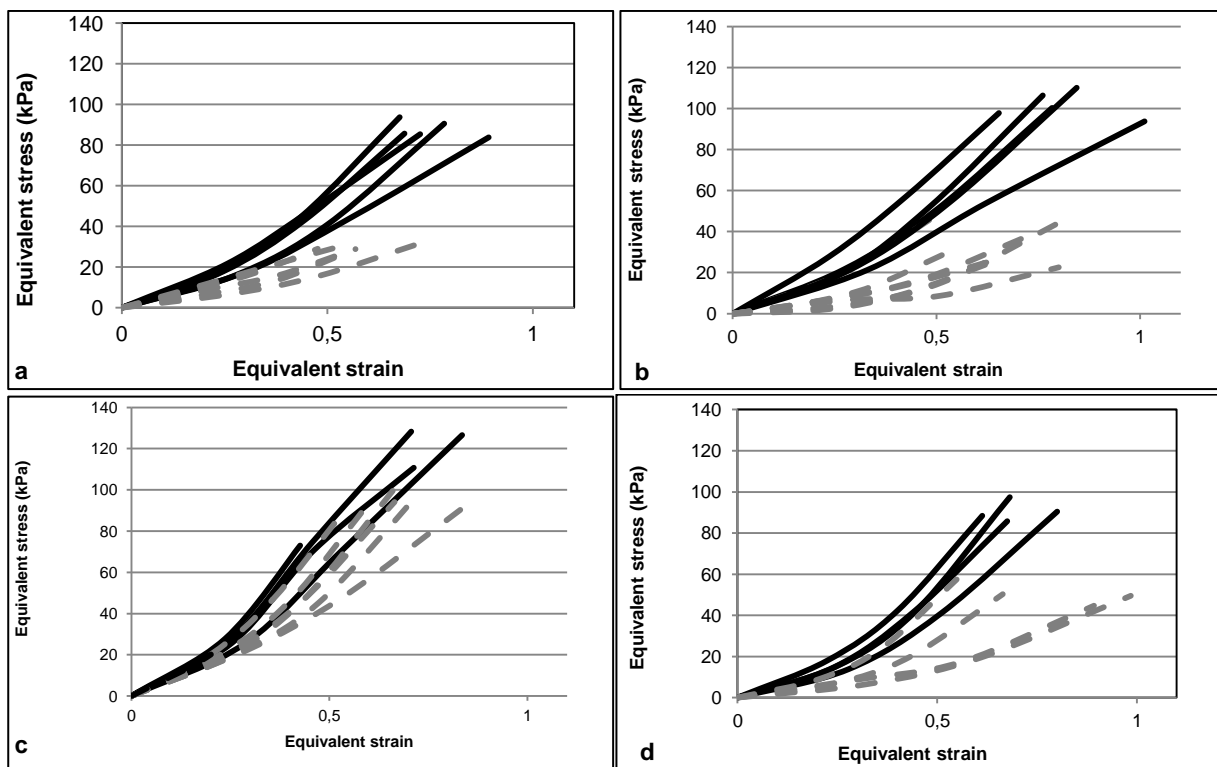
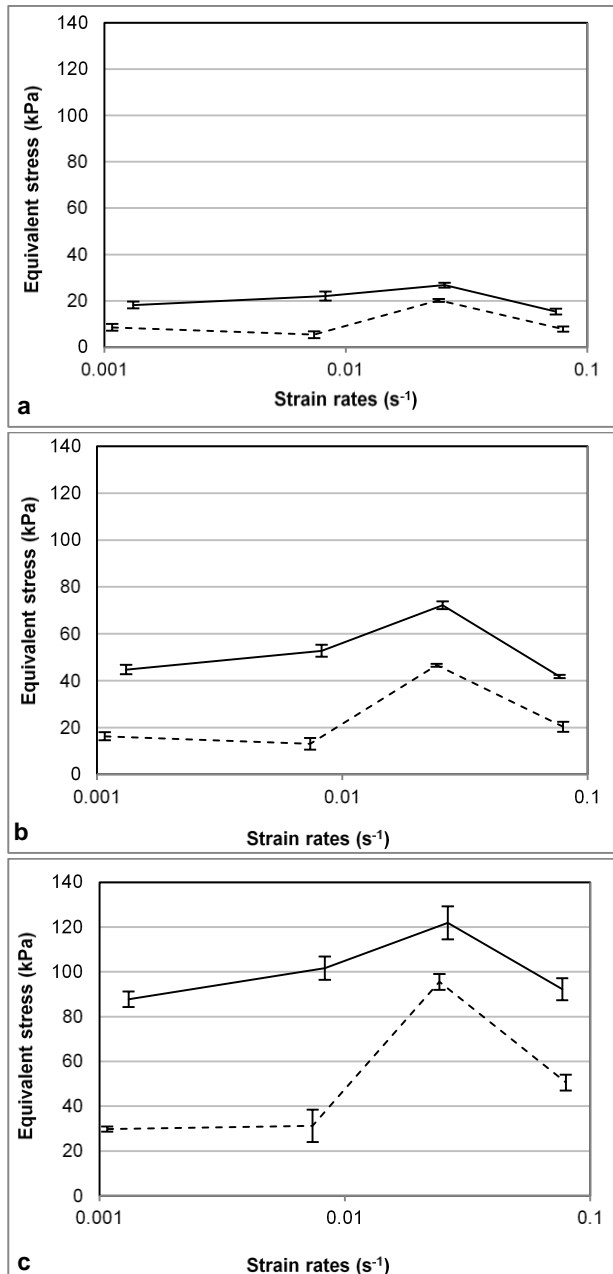


Figure 6. Mechanical behavior of sprayed and molded alginate hydrogels at different velocity. Plane Strain Compression Test (PSC test) was performed on several calcium gelled alginate hydrogel (1.5%) to obtain equivalent stress as a function of equivalent strain. Sprayed alginate was represented by continuous lines and molded alginate was represented by discontinuous lines, at different controlled velocity: 0.1 mm min^{-1}

(a), 0.6 mm min⁻¹ (b), 2 mm min⁻¹ (c) and 6 mm min⁻¹ (d). Each experiment was performed and analyzed using 4 tests and each curve corresponds to one specimen.

Furthermore, the influence of the preparation method of the alginate hydrogel can be more clearly illustrated by the stress-strain curves as a function of the strain rate, at different compression displacements (Fig. 7a, b and c for $\delta(t) = 0.3, 0.5$ and 0.7 mm respectively). Moreover, as mechanical behavior depends on the compression stress and specimens thickness, we choose to represent strain rate, to avoid differences due to this parameters. For each compression displacement, $\delta(t)$, the equivalent stress values were higher for S (continuous lines) than for M (discontinuous lines). At a fixed level of $\bar{\epsilon}$, values for $\bar{\sigma}$ increased with $\delta(t)$, and on the other hand, for the same $\delta(t)$, $\bar{\sigma}$ increased with $\bar{\epsilon}$ up to a strain-rate $\dot{\epsilon} = 0.025$ s⁻¹ and then decreased. So, for S gel specimens tested at $\delta(t) = 0.5$ mm, $\bar{\sigma}$ increased from 44.7 kPa to 72.2 kPa up to $\dot{\epsilon} = 0.025$ s⁻¹, and then decreased to 41.8 kPa. The same strain-rate effect was observed for the M specimens.

The physical interpretation of this phenomenon is not yet clearly elucidated. This particular configuration is sensitive to friction at the surface of the specimens, but limited thanks to the use of smooth anvils and to the high water content of this scaffold. Let us note however, that this high strain-rate of 0.079 s⁻¹ could roughly correspond to the case of a violent impact on the articular cartilage, at the level of the knee, as in the case of a jump from a chair, according to Eckstein.⁵⁷



From this viewpoint, the biomaterial behavior could be described as viscoplastic for large strains. The alginate mechanical behavior was analyzed taking into account morphology, distribution and interaction of alginate molecular chain.⁵⁸ However, despite this last point, the stress performances of the sprayed biomaterials (at a pressure of 0.9 bar) are higher than for the molded ones. This report is checked whatever the strain rate and the level of deformation.

Moreover, the range of the observed stress amplitude is in accordance with what other authors have found about this kind of biomaterials, (Table 1).^{58, 59} Moreover, the stress-strain curves have the same appearance, but with a strain of 50% at failure at 120 mm min⁻¹, against 80% at 6 mm min⁻¹ for our results. Table 1 enables us to compare our mechanical results with those of Mancini et al. and Moresi et al., obtained on the same sodium alginate (medium viscosity from Sigma), but in non-pressure-sealed conditions (non-autoclaved).^{58, 59} Note that non-autoclaved sodium alginates have a higher viscosity than the autoclaved ones (data not shown).

Figure 7. Stress response as a function of the compression displacement: 0.3 mm (a), 0.5 mm (b) and 0.7 mm (c) for sprayed (continuous lines) or molded alginate hydrogel (discontinuous lines). For all compression displacements, the maximal equivalent stress corresponds to a controlled strain-rate 0.023 s^{-1} at 2 mm min^{-1} . The results were expressed in means \pm SEM ($n = 10$ for each strain-rate level).

Table 1. Mechanical properties of sodium alginate gel (medium viscosity, Sigma) in different studies.

Study	Type of mechanical test	Gel alginate (% w/v)	Stress at failure (kPa)	Strain at failure	Dimensions of the specimens (mm)
Mancini et al. ⁵⁸	uniaxial compression test at strain-rate 0.08 s^{-1} (cylindrical specimens) non autoclaved	1.50	$\sigma_{\text{engineering}}: 201.3^{\pm 0.2}$ $\sigma_{\text{true}}: 312$	$\epsilon_{\text{engineering}}: 0.55^{\pm 0.01}$ $\epsilon_{\text{true}}: 0.44$	$H_0 = 24.7^{\pm 0.10}$ $D_0 = 23.4$
Moresi et al. ⁵⁹	confined compression test at strain-rate 0.08 s^{-1} (cylindrical specimens) non autoclaved	1.25	$\sigma_{\text{true}}: 76.3^{\pm 2}$	$\epsilon_{\text{true}}: 0.83^{\pm 0.01}$	$H_0 = 25$ $D_0 = 25$
Present work	plane strain compressive tests at strain-rate 0.069 s^{-1} (sprayed plane specimens) autoclaved	1.50	$\sigma_{\text{true}}: 100^{\pm 20}$	$\epsilon_{\text{true}}: 0.80^{\pm 0.20}$	$2h_0 = 1.47^{\pm 0.10}$ $L_0 = 28$

Conclusion:

We have shown that chondrocytes seeded in sodium alginate hydrogel may produce a buildup of sprayed biomaterials *in vitro* and lead to the reconstruction of a biological tissue. We report here the first demonstration of sprayed mixed alginate hydrogel and chondrocytes without damage for cells during long term culture. We demonstrated clearly, that the sprayed biomaterial (at 0.9 bar) does not only keep the mechanical properties needed for cells, but also maintains the chondrocyte phenotype and the capacity to induce cartilage. This original strategy could be used to design new stratified engineered tissues through progressive cells and hydrogel, spraying alternate with polyelectrolyte to weld layers- which is unrealizable with the molding method. This spraying process contributes to form a highly functional and structured biomaterial able to maintain chondrocyte phenotype for cartilage regeneration.

Acknowledgement:

This work was supported by the project ANR06-BLAN-0197-01/CartilSpray, from the “Agence Nationale de la Recherche”, the “Fondation Avenir”. This work was also supported by the “Lorraine region” grant. N. Jessel is indebted to CHU de Nancy, Hôpital Central, orthopedic surgery (Contrat d’interface INSERM-CHU). The authors would like to thank Dr J.C. VOEGEL for fellowship support, T. Fortin for his help and the laboratory of immunology (Pr FAURE and Pr BENET) for giving us access to the cytometer. Confocal microscopy pictures were obtained thanks to the “plate forme imagerie cellulaire PTIBC – IBISA”.

References

1. R. Langer and J. P. Vacanti, *Science*, 1993, **260**, 920-926.

2. M. Wong and D. R. Carter, *Bone*, 2003, **33**, 1-13.
3. A. C. Shieh and K. A. Athanasiou, *J Biomech*, 2006, **39**, 1595-1602.
4. J. A. Buckwalter and H. J. Mankin, *Instr Course Lect*, 1998, **47**, 477-486.
5. E. B. Hunziker, T. M. Quinn and H. J. Hauselmann, *Osteoarthritis Cartilage*, 2002, **10**, 564-572.
6. C. Chung and J. A. Burdick, *Adv Drug Deliv Rev*, 2008, **60**, 243-262.
7. E. Han, W. C. Bae, N. D. Hsieh-Bonassera, V. W. Wong, B. L. Schumacher, S. Gortz, K. Masuda, W. D. Bugbee and R. L. Sah, *Clin Orthop Relat Res*, 2008, **466**, 1912-1920.
8. M. M. Stevens and J. H. George, *Science*, 2005, **310**, 1135-1138.
9. L. L. Hench and J. M. Polak, *Science*, 2002, **295**, 1014-1017.
10. J. D. Kretlow and A. G. Mikos, *Tissue Eng*, 2007, **13**, 927-938.
11. C. Liu, Z. Xia and J. T. Czernuszka, *Chemical Engineering Research and Design*, 2007, **85**, 1051-1064.
12. C. Z. Liu and J. T. Czernuszka, *Materials Science and Technology*, 2007, **23**, 379-391.
13. N. S. Hwang, S. Varghese, H. J. Lee, P. Theprungsirikul, A. Canver, B. Sharma and J. Elisseeff, *FEBS Lett*, 2007, **581**, 4172-4178.
14. T. Akaike, T. Okano, M. Akashi, M. Terano, N. Yui and editors, *Advances in Polymeric Biomaterials Science*. Tokyo CMC Co. Ltd, 1997, 355-362.
15. W. Knoll, *Curr Opin Colloid Interface Sci.*, 1996, **1**, 137-143.
16. P. T. Hammond, *Curr Opin Colloid Interface Sci.*, 2000, **4**, 430-442.
17. P. Bertrand, A. Jonas, A. Laschewsky and R. Legras, *Macromolecular Rapid Communications*, 2000, **21**, 319-348.
18. G. M. Williams, T. J. Klein and R. L. Sah, *Acta Biomater*, 2005, **1**, 625-633.
19. Y. Wang, N. de Isla, C. Huselstein, B. Wang, P. Netter, J. F. Stoltz and S. Muller, *Biomed Mater Eng*, 2008, **18**, S47-54.
20. C. S. Lee, J. P. Gleghorn, N. Won Choi, M. Cabodi, A. D. Stroock and L. J. Bonassar, *Biomaterials*, 2007, **28**, 2987-2993.
21. K. W. Ng, C. C. B. Wang, R. L. Mauck, T.-A. N. Kelly, N. O. Chahine, K. D. Costa, G. A. Ateshian and C. T. Hung, *Journal of Orthopaedic Research*, 2005, **23**, 134-141.
22. C. Picart, A. Schneider, O. Etienne, J. Mutterer, P. Schaaf, C. Egles, N. Jessel and J. C. Voegel, *Advanced Functional Materials*, 2005, **15**, 1771-1780.
23. N. B. Jessel, P. Schwinté, R. Donohue, P. Lavalley, F. Boulmedais, R. Darcy, B. Szalontai, J. C. Voegel and J. Ogier, *Advanced Functional Materials*, 2004, **14**, 963-969.
24. N. Benkirane-Jessel, P. Lavalley, E. Hübsch, V. Holl, B. Senger, Y. Haïkel, J. C. Voegel, J. Ogier and P. Schaaf, *Advanced Functional Materials*, 2005, **15**, 648-654.
25. N. Jessel, F. Atalar, P. Lavalley, J. Mutterer, G. Decher, P. Schaaf, J. C. Voegel and J. Ogier, *Advanced Materials*, 2003, **15**, 692-695.
26. N. Benkirane-Jessel, P. Lavalley, F. Meyer, F. Audouin, B. Frisch, P. Schaaf, J. Ogier, G. Decher and J. C. Voegel, *Advanced Materials*, 2004, **16**, 1507-1511.
27. P. Schultz, D. Vautier, L. Richert, N. Jessel, Y. Haikel, P. Schaaf, J.-C. Voegel, J. Ogier and C. Debry, *Biomaterials*, 2005, **26**, 2621-2630.

28. J. M. Garza, N. Jessel, G. Ladam, V. Dupray, S. Muller, J. F. Stoltz, P. Schaaf, J. C. Voegel and P. Lavalle, *Langmuir*, 2005, **21**, 12372-12377.
29. S. C. Gangloff, G. Ladam, V. Dupray, K. Fukase, K. Brandenburg, M. Guenounou, P. Schaaf, J. C. Voegel and N. Jessel, *Biomaterials*, 2006, **27**, 1771-1777.
30. L. Richert, A. Schneider, D. Vautier, C. Vodouhe, N. Jessel, E. Payan, P. Schaaf, J. C. Voegel and C. Picart, *Cell Biochem Biophys*, 2006, **44**, 273-285.
31. N. Jessel, M. Oulad-Abdelghani, F. Meyer, P. Lavalle, Y. Haikel, P. Schaaf and J. C. Voegel, *Proc Natl Acad Sci U S A*, 2006, **103**, 8618-8621.
32. A. Dierich, E. Le Guen, N. Messaddeq, J. F. Stoltz, P. Netter, P. Schaaf, J. C. Voegel and N. Benkirane-Jessel, *Advanced Materials*, 2007, **19**, 693-697.
33. X. Zhang, K. K. Sharma, M. Boeglin, J. Ogier, D. Mainard, J.-C. Voegel, Y. Meïly and N. Benkirane-Jessel, *Nano Letters*, 2008, **8**, 2432-2436.
34. L. Grossin, D. Cortial, B. Saulnier, O. Félix, A. Chassepot, G. Decher, P. Netter, P. Schaaf, P. Gillet, D. Mainard, J.-C. Voegel and N. Benkirane-Jessel, *Advanced materials*, 2009, **21**, 650-655.
35. N. Benkirane-Jessel, P. Schwinté, P. Falvey, R. Darcy, Y. Haïkel, P. Schaaf, J. C. Voegel and J. Ogier, *Advanced Functional Materials*, 2004, **14**, 174-182.
36. W. Tan and T. A. Desai, *Biomaterials*, 2004 **25**, 1355-1364.
37. W. S. Veazey, K. J. Anusavice and K. Moore, *Journal of Biomedical Materials Research Part B: Applied Biomaterials*, 2005, **72B**, 334-338.
38. N. Matsuda, T. Shimizu, M. Yamato and T. Okano, *Advanced Materials*, 2007, **19**, 3089-3099.
39. M. Matsusaki, K. Kadowaki, Y. Nakahara and M. Akashi, *Angewandte Chemie International Edition*, 2007, **46**, 4689-4692.
40. Y. Nahmias, A. Arneja, T. T. Tower, M. J. Renn and D. J. Odde, *Tissue Eng*, 2005, **11**, 701-708.
41. I. Grant, K. Warwick, J. Marshall, C. Green and R. Martin, *British Journal of Plastic Surgery*, 2002, **55**, 219-227.
42. F. A. Navarro, M. L. Stoner, H. B. Lee, C. S. Park, F. M. Wood and D. P. Orgill, *J Burn Care Rehabil*, 2001, **22**, 41-46.
43. A. T. Hafez, D. J. Bägli, A. Bahoric, K. Aitken, C. R. Smith, D. Herz and A. E. Khoury, *The Journal of Urology*, 2003, **169**, 2316-2320.
44. H. J. Kong, M. K. Smith and D. J. Mooney, *Biomaterials*, 2003, **24**, 4023-4029.
45. G. D. Nicodemus and S. J. Bryant, *J Biomech*, 2008, **41**, 1528-1536.
46. M. Wong, M. Siegrist, X. Wang and E. Hunziker, *J Orthop Res*, 2001, **19**, 493-499.
47. S. C. N. Chang, J. A. Rowley, G. Tobias, N. G. Genes, A. K. Roy, D. J. Mooney, C. A. Vacanti and L. J. Bonassar, *Journal of Biomedical Materials Research*, 2001, **55**, 503-511.
48. H. Mjahed, C. Porcel, B. Senger, A. Chassepot, P. Netter, P. Gillet, G. Decher, J.-C. Voegel, P. Schaaf, N. Benkirane-Jessel and F. Boulmedais, *Soft matter*, 2008, **4**, 1422-1429.

49. M. Moresi, M. Mancini, M. Bruno and R. Rancini, *Journal of Texture Studies*, 2001, **32**, 375-396.
50. A. Nussinovitch, M. Peleg and M. D. Normand, *Journal of Food Science*, 1989, **54**, 1013-1016.
51. P. Montmitonnet, F. Delamare and B. Rizoulières, *Wear*, 2000, **245**, 125-135.
52. K. Masaki, Y. S. Sato, M. Maeda and H. Kokawa, *Scripta Materialia*, 2008, **58**, 355-360.
53. B. Grigolo, L. De Franceschi, L. Roseti, L. Cattini and A. Facchini, *Biomaterials*, 2005, **26**, 5668-5676.
54. J. E. Jeffrey, D. W. Gregory and R. M. Aspden, *Arch Biochem Biophys*, 1995, **322**, 87-96.
55. M. Kino-oka, Y. Morinaga, M. H. Kim, Y. Takezawa, M. Kawase, K. Yagi and M. Taya, *Biomaterials*, 2007, **28**, 1680-1688.
56. D. E. Shepherd and B. B. Seedhom, *Ann Rheum Dis*, 1999, **58**, 27-34.
57. F. Eckstein, B. Lemberger, C. Gratzke, M. Hudelmaier, C. Glaser, K. H. Englmeier and M. Reiser, *Ann Rheum Dis*, 2005, **64**, 291-295.
58. M. Mancini, M. Moresi and R. Rancini, *Journal of Food Engineering*, 1999, **39**, 369-378.
59. M. Moresi and M. Bruno, *Journal of Food Engineering*, 2007, **82**, 298-309.

